

## Investigations of low $q_a$ discharges in the SINP tokamak

S LAHIRI\*, A N S IYENGAR, S MUKHOPADHYAY and R PAL

Saha Institute of Nuclear Physics, 1/AF, Bidhannagar, Kolkata 700 064, India

\*Present address: Techno India Institute of Technology, EM-4, Sector V, Salt Lake City, Kolkata 700 091, India

MS received 26 June 2000; revised 13 July 2001

**Abstract.** Low edge safety factor discharges including very low  $q_a$  ( $1 < q_a < 2$ ) and ultra low  $q_a$  ( $0 < q_a < 1$ ) have been obtained in the SINP tokamak. It has been observed that accessibility of these discharges depends crucially on the fast rate of plasma current rise. Several interesting results in terms of different time scales like  $T_{q_a}$ ,  $\tau_R$  etc have been obtained using a set of softwares developed at SINP. From fluctuation analysis of the external magnetic probe data it has been found that MHD instabilities  $m = 1, n = 1$  and  $m = 2, n = 1$  etc. play major role in the evolution of these discharges. To investigate the internal details of these discharges, an internal magnetic probe system has been developed using which current density  $j_\phi$  and other related parameters have been estimated. By carrying out a resistive stability analysis, evidence of the above-mentioned MHD instabilities have again been found. The physical processes lying behind the accessibility and evolution of the low  $q_a$  discharges have been thoroughly investigated.

**Keywords.** Safety factor; tokamak; current density; MHD; stability.

**PACS No.** 52.55.Fa

### 1. Introduction

Discharges with a wide range of edge safety factors ( $0 < q_a < 5.0$ ) [1–4] have been obtained in the SINP tokamak. This range includes the normal  $q_a$  (NQ), very low  $q_a$  (VLQ) and ultra low  $q_a$  (ULQ) discharges. The low  $q_a$  (LQ) discharges [5–8], especially the ULQ discharges [9–11] have been obtained in a very small number of machines throughout the world. Moreover, the low  $q_a$  discharges are considered to be beneficial and interesting from both technological and physical point of view [4]. Thus, the physical processes lying behind the accessibility and evolution of these discharges are still interesting phenomena to be studied. In this paper we are going to present some of the results obtained from several experimental and numerical investigations carried out in relation to the accessibility and evolution of the low  $q_a$  regime in the SINP tokamak.

## 2. Experiments and results related to the accessibility of the low $q_a$ discharges

It is possible to access the low  $q_a$  regime in the SINP tokamak by carrying out a systematic and detailed study of various operating parameters. Details of this tokamak and the experiments have already been published in various works [1–4,12]. The low  $q_a$  discharges have been obtained in a specific parameter space as follows: limiter radius ( $a_l$ ) from 0.065 m to 0.045 m,  $B_t$  from 0.44 T to 0.33 T, secondary voltage from  $\approx 60$  V to  $\approx 90$  V and gas filling pressure ( $P_{\text{fill}}$ )  $\geq 3.0 \times 10^{-4}$  torr. In these experiments, the base pressure was kept at  $\approx 2 \times 10^{-7}$  torr. Only some low power discharges were carried out for the conditioning of the vessel. We have used loop voltage coil, Rogowskii coil, Mirnov coils, hard X-ray detection system etc in these experiments.

Our results indicate that one of the main reasons for getting low  $q_a$  discharges in the SINP tokamak is the fast rate of rise of the plasma current. Factors such as the low toroidal field and high gas filling pressure also have important contributions. Some other factors like presence of the conducting shell [2,3], surrounding the vacuum vessel, may also have some contribution in the setting up process. Loop voltage, plasma current ( $I_p$ ) and the edge safety factor  $q_a$  for a typical ULQ discharge are shown in figures 1a, 1b and 1c respectively. It is seen that  $I_p$  rises very fast and also linearly up to  $250 \mu\text{s}$  and at this time a positive jump in the loop voltage is observed. This positive jump is sustained up to  $350\text{--}400 \mu\text{s}$ . Immediately after this positive jump, rate of rise of the plasma current ( $\dot{I}_p$ ) falls considerably.

Using data analysis software developed during the present work, a vast amount of data collected from more than thousand low  $q_a$  discharges have been analysed in detail. One such software is ‘ANDIS’ (ANalysis of DIScharge) which can calculate the time evolution, carry out peak analysis etc. of almost 30 plasma parameters with or without user intervention in a very short time ( $< 2$  min). Several time scales (Alfven time ( $\approx \mu\text{s}$ ), confinement time ( $\approx 50 \mu\text{s}$ ), current rise time ( $> 1$  ms), MHD time ( $\approx 50 \mu\text{s}$ ), resistive diffusion time  $\tau_R$  ( $\approx 300 \mu\text{s}$ ), time to cross different  $q_a$  barriers  $T_{q_a}$  (varies from  $200 \mu\text{s}$  to  $500 \mu\text{s}$ )) etc. have been studied in detail in relation to the accessibility of the low  $q_a$  discharges obtained in our machine. Interesting results in terms of effective plasma resistivity ( $\eta^*$ ),  $\tau_R$ ,  $T_{q_a}$  etc. have been obtained [4,12]. The most important among these is as follows: if the relation

$$\frac{T_{q_a+1}}{\tau_R} < 1 \quad (1)$$

holds, it is possible to cross the mode rational surface barrier represented by  $q_a$ , where  $q_a + 1$  represents the previous mode rational surface barrier. For example if  $(T_{1.5}/\tau_R) < 1$ , the  $q_a = 1$  barrier can be crossed and the discharge enters into the ULQ regime [4]. Details of these results have already been published [4].

In the initial current rise phase, plasma current is almost linear. Using this and from the definition of  $q_a$  ( $q_a = 2\pi a_p^2 B_t / \mu_0 R I_p$ ) ( $I_p = (I_p/T_{q_a})T_{q_a} = \dot{I}_p T_{q_a}$ ), we have obtained a general relation for  $T_{q_a}$  (the time to cross the rational  $q_a$  values) [3]

$$\frac{T_{q_a}}{B_t} = \frac{a_p^2 2\pi}{\mu_0 R q_a} \dot{I}_p^{-1}, \quad (2)$$

where  $B_t$  is the toroidal field,  $a$  and  $R$  are the minor and major radii respectively. Now, for  $q_a = 2$  one can get the relation between  $T_2/B_t$  and  $\dot{I}_p^{-1}$  as given in [13]. For  $q_a = 1$ , the relation between  $T_1/B_t$  and  $\dot{I}_p^{-1}$  is as follows:

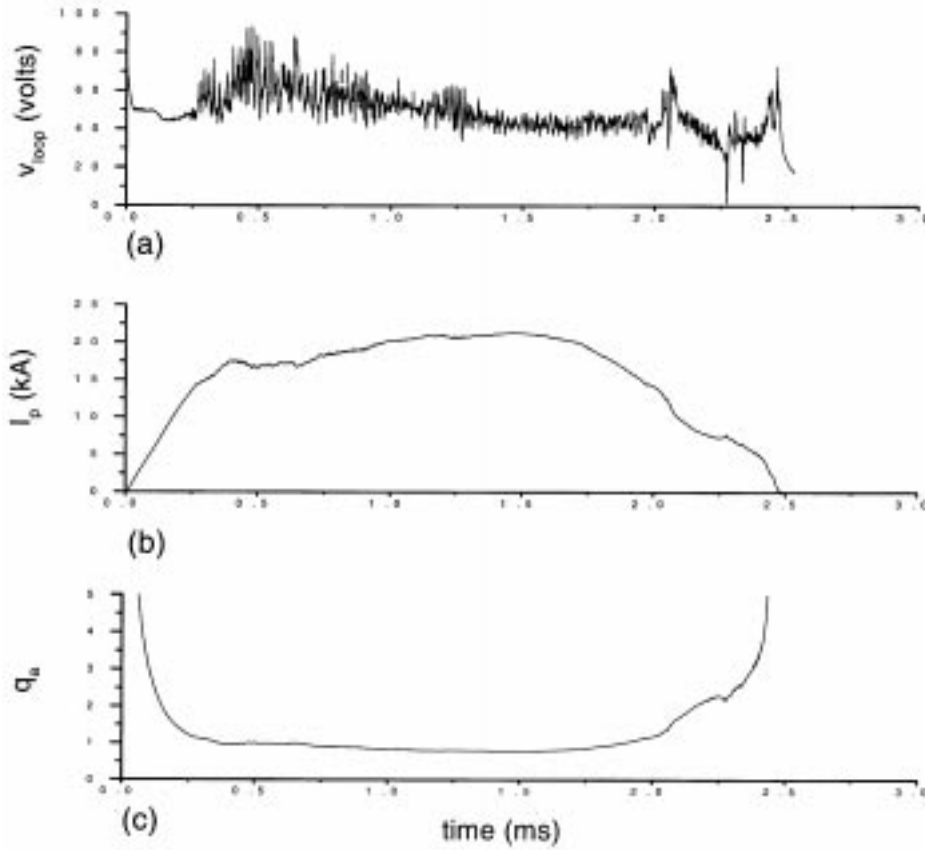


**Figure 1.** (a) Loop voltage, (b) plasma current, (c) edge safety factor of an ULQ discharge.

$$\frac{T_1}{B_t} (\mu\text{s/kG}) = \frac{1}{2.0 \times 10^{-12}} \times \frac{a_p^2}{RI_p}. \quad (3)$$

In order to compare the experimentally obtained data with eq. (3), we have plotted  $T_1/B_t$  vs.  $a_p^2 I_p^{-1}$  as a scatter plot (figure 2). Carrying out a least square fit for this scatter plot, we have obtained the relation [14]

$$\frac{T_1}{B_t} (\mu\text{s/kG}) \approx \frac{1}{3.305 \times 10^{-12}} \frac{a_p^2}{RI_p} + 30.72. \quad (4)$$

Considering eq. (1) and also the condition  $\eta^* B_t = \text{constant} \approx 4.5 \mu\Omega \text{ mT}$  (where  $\eta^*$  = plasma effective resistivity =  $\mu_0 a^2 / \tau_R$ ) it has been possible to get the equation

$$I_p > \frac{C}{R(q_a + 1)}, \quad (5)$$

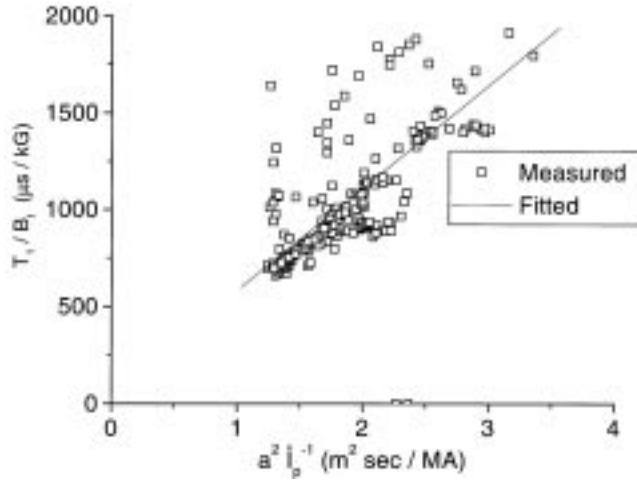


Figure 2.  $(T_i/B_i)$   $\mu\text{s/kG}$  vs.  $a^2 I_p^{-1}$   $\text{m}^2\text{s/MA}$ .

where  $C = 1.8 \times 10^7$  Amp m/s. From eq. (5) it is clear that the required value of the rate of rise of the plasma current to cross the mode rational barrier represented by  $q_a$  varies inversely with the value of  $q_a$  itself and the major radius of the tokamak. For a particular tokamak, since the major radius  $R$  is constant, the required rate of rise depends only on the value of the mode rational barrier to be crossed. The minimum  $\dot{I}_p$  in getting low  $q_a$  discharges have been found to be  $\dot{I}_p \geq 22$  MA/s for VLQ and  $\dot{I}_p \geq 30$  MA/s for ULQ [12]. Runaway electrons have also been found to take part in determining the accessibility of the low  $q_a$  discharges [15]. These relations establish the fact that the low  $q_a$  discharges obtained in the SINP tokamak fall in the general pattern of low  $q_a$  discharges obtained in other machines, where low  $q_a$  discharges are possible. In other words, the accessibility of the low  $q_a$  discharges depend on certain parameters like  $\dot{I}_p$ , gas filling pressure  $P_{\text{fill}}$ ,  $B_t$  and limiter radius  $a$  etc. It has also been found that the required  $\dot{I}_p$  to get low  $q_a$  discharges is bounded in the parameter space by a minimum value of the gas filling pressure ( $P_{\text{fill}}$ ) as was obtained in Repute-1 [13]. This minimum required  $\dot{I}_p$  is inversely proportional to  $P_{\text{fill}}$ . In Repute-1,

$$\dot{I}_p (\text{As}^{-1}) \geq 5 \times \frac{10^6}{P_{\text{fill}} (\text{mtorr})} \quad (6)$$

was obtained [13] whereas in the SINP tokamak

$$\dot{I}_p (\text{As}^{-1}) > \frac{10^7}{P_{\text{fill}} (\text{mtorr})} \quad (7)$$

was obtained. This scaling is in agreement with the conventional understanding that the current ramp up has to be rapid enough to achieve low  $q_a$  (both VLQ and ULQ) discharges and low  $q_a$  operations can be obtained rather easily with higher  $P_{\text{fill}}$ .

From the external magnetic coils, we have estimated the evolution of the MHD instabilities in the current rise phase of the low  $q_a$  discharges by using another software developed,

namely MASA (MAGnetic Signal Analysis). This software relies heavily on correlation and spectral techniques. It has been observed that  $m = 2, n = 1$  instability plays a major role in the VLQ discharges. In the ULQ discharges, the  $m = 1, n = 1$  instability plays a similar role. In addition, for the latter discharges, the  $m = 3, n = 2$  mode also seem to have some role. It seems that the large positive spike observed in the loop voltage is a direct consequence of these instabilities.

The above results relating to the accessibility of low  $q_a$  discharges in the SINP tokamak led to the following conjectures:

- Due to large  $\dot{I}_p$ , the toroidal current density ( $j_\phi$ ) profile remains hollow for a considerable period of time. Such a profile is known to be resilient to instabilities important in the low  $q_a$  regime. Thus, the discharge gets enough time to increase  $I_p$  and access the low  $q_a$  regime.
- Due to large  $\dot{I}_p$ , the instabilities do not get enough time to grow because the related resonant surface is lost within a very short time.

As a consequence, the resulting amplitude of the instabilities remain small and the plasma survives even in the low  $q_a$  operating regime. In order to verify our conjectures, we carried out experiments to find out the internal structure of the plasma.

### 2.1 *Experiments and results related to the evolution of the discharge*

For a low temperature, small tokamak device, an internal magnetic probe (IMP) is known to be a good diagnostic for elaborate measurements and are widely used for similar purposes. We designed and fabricated an internal magnetic probe array consisting of ten pickup coils. Each of these coils is  $3 \times 4 \text{ mm}^2$  in cross-section and are wound on a teflon strip. The teflon strip is inserted inside a quartz tube of 6 mm inner diameter and 8 mm outer diameter. The frequency response of the coils were measured to be 100 kHz. This response sufficed our purposes because we were mostly interested in the MHD fluctuations which are known to lie below 100 kHz. In order to avoid ground loop problems, ends of the coils were tightly twisted and connected to a set of differential amplifiers. The array could be inserted inside the tokamak vessel from a vertical or a horizontal port. The schematic diagram of the internal magnetic probe system is shown in figure 3a. The placement of the probe inside the vacuum vessel is plotted in figure 3b. Using the same probe coil windings (A), poloidal ( $B_\theta$ ) and toroidal ( $B_\phi$ ) magnetic field profiles were measured depending on the orientation of the coils. There is also a provision for measuring radial magnetic field ( $B_r$ ) using the set of coils (B) shown in figure 3a. We have measured the poloidal magnetic field ( $B_\theta$ ) at discrete spatial points using this probe applying Faraday's law of induction which can be written as  $\partial\Phi/\partial t = \text{induced e.m.f.}$ , where  $\Phi$  is the magnetic flux.

Evolution of the toroidal current density profile ( $j_\phi$ ) is obtained in two steps: (i) the temporal evolution of  $B_\theta$  profile is reconstructed from the discrete measured values of  $B_\theta$ , (ii) assuming cylindrical symmetry, the temporal evolution of  $j_\phi$  is obtained using

$$j_\phi = \frac{1}{\mu_0 r} \frac{d}{dr}(rB_\theta). \quad (8)$$

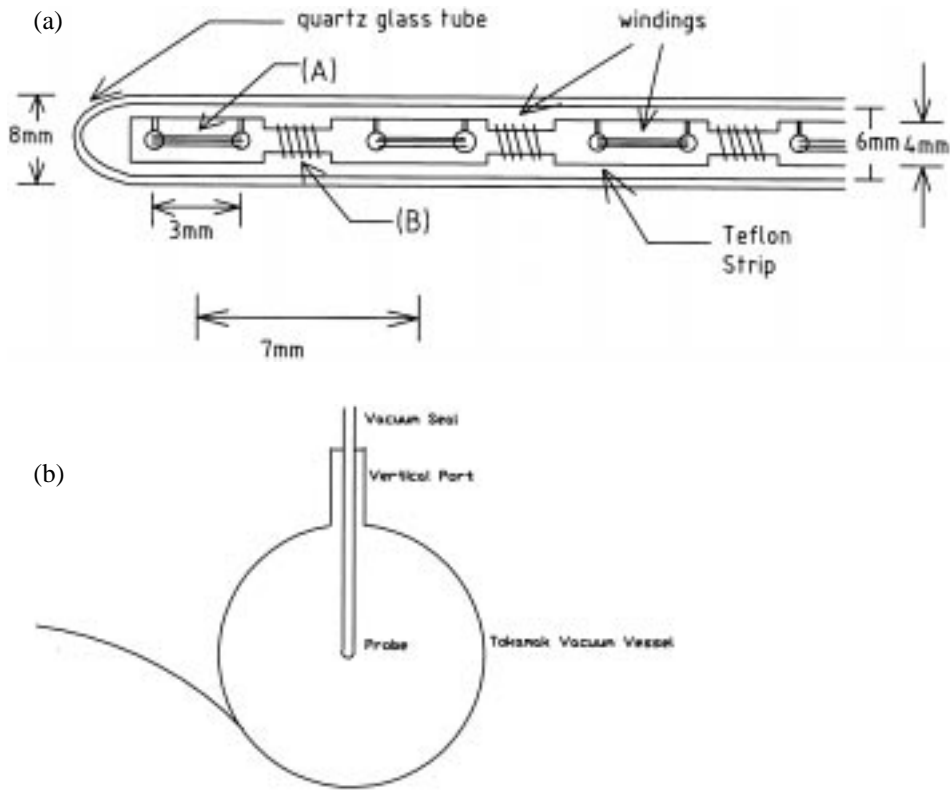


**Figure 3.** (a) Schematic diagram of the internal magnetic probe. A – direction of winding for measuring  $B_\theta/B_\phi$ , B – direction of winding for measuring  $B_r$ . (b) Placement of the internal magnetic probe inside the tokamak vessel.

Both the above are accomplished using the software ‘REPRO’ which is the abbreviation of the words ‘REconstruction of PROfiles’. This user friendly software is written by us during the course of this work.

In the toroidal system the plasma column normally experiences a horizontal shift. Accordingly, we have corrected the field profiles so that we can plot them not as a function of the geometrical minor radius, but as a function of the radial coordinate, whose origin is the shifted axis of the displaced flux surfaces [16]. The polynomial fitting of the uncorrected field components are

$$B_\theta(r) = \sum_{j=0}^n a_j r^{(2j+1)}. \quad (9)$$

The corrected field profiles (valid for small shifts) may in fact be written as

$$B_\theta(r) = \sum_{j=0}^n a_j \left(1 - \frac{j\Delta^2}{r^2}\right) r^{2j+1}, \quad (10)$$

where  $\Delta$  is the central plasma displacement. At this point it should be mentioned that in the cold plasma like ours the shift of the plasma column is small ( $< 5$  mm). The coefficients of the polynomials ( $a_j$ ) are evaluated in the least-square sense using the singular value decomposition (SVD) technique. During fitting  $B_\theta$ , it was considered that  $B_\theta = 0$  at  $r = 0$  and it is equal to  $\mu_0 I_p / 2\pi a_p$  at  $r = a_p$ . The temporal evolution of these properties ( $B_\theta$ ,  $j_\phi$  etc.) have been obtained automatically by carrying out the analysis once after each  $\Delta t$ , where  $\Delta t$  is a desired time gap.

The fitted  $B_\theta$  profiles in the rising phase of the discharge are shown in figure 4a at 210  $\mu\text{s}$  and 560  $\mu\text{s}$  after the initiation of the discharge. Evolution of  $j_\phi(r)$  and  $q(r)$  profiles typically found in the rising phase of an ULQ discharge are shown in figures 4b and 4c respectively. At 210  $\mu\text{s}$  after the initiation of the discharge,  $j_\phi(r)$  profile was hollow (figure 4b) and the corresponding  $q(r)$  profile shows negative shear (figure 4c). At 560  $\mu\text{s}$ , the  $j_\phi(r)$  profile (figure 4b) is parabolic and so the  $q(r)$  profile (figure 4c) changes to a monotonic shape. More detailed equilibrium reconstructions using a Grad–Shafranov solver (once again, developed during the course of the present investigation), was found to yield similar results as regards the  $j_\phi(r)$  and  $q(r)$  profiles. The  $j_\phi(r)$  profile in a low  $q_a$  discharge was found to remain hollow up to the positive jump in the loop voltage signal. After that it was found to change to a parabolic shape indicating the penetration of current towards the center of the plasma column. The  $j_\phi$  profile shape changes from hollow to a parabolic one in a time scale of the order of resistive diffusion time (350–400  $\mu\text{s}$ ) in the low  $q_a$  discharges obtained in this machine. We also mentioned that an important relation between  $T_{q_a}$  and  $\tau_R$  [4] had been obtained in our case. So, we think that the  $\tau_R$  is one of the most important time scales related to the low  $q_a$  discharges obtained in the SINP tokamak.

Thus, it was possible to experimentally verify our first conjecture regarding the shape of the current density profile in the low  $q_a$  discharges. It is seen that the  $j_\phi(r)$  profile remains hollow till  $q_a \approx 1.33$  for ULQ discharges and  $q_a \approx 2.0$  for the VLQ discharges.

## 2.2 Stability analysis

In order to verify our second conjecture, we carried out detailed stability analysis of the LQ discharges in the current rise phase. With this goal in mind, we have developed a one-dimensional resistive stability analysis code which can handle multiple resonant surfaces [17]. Using the current density profiles obtained experimentally, we calculated the growth rates ( $\gamma$ ) of a large number of MHD modes. At this point it should be mentioned that the external magnetic probe coils in the SINP tokamak are very few (only four in the poloidal direction). Moreover, since they are quite far from the plasma (even outside the vessel), it is difficult to accurately diagnose the onset, duration and the growth rate of the MHD modes using the external coils only. This is specially true for the instabilities residing in the inner region of the plasma. So, this stability analysis code is very important in our case. From these growth rates and the duration for which the relevant resonant surfaces existed, it was possible to find out the effect of these MHD modes. For example, the estimated growth time ( $1/\gamma$ ) of various modes at early rising phase, before the positive jump in the loop voltage and around that jump for an ULQ discharge are written in tables 1, 2 and 3 respectively. The  $j_\phi(r)$  profile shape was hollow in the early rising phase, less hollow just before the positive jump in the loop voltage and around the positive jump it was of parabolic shape.

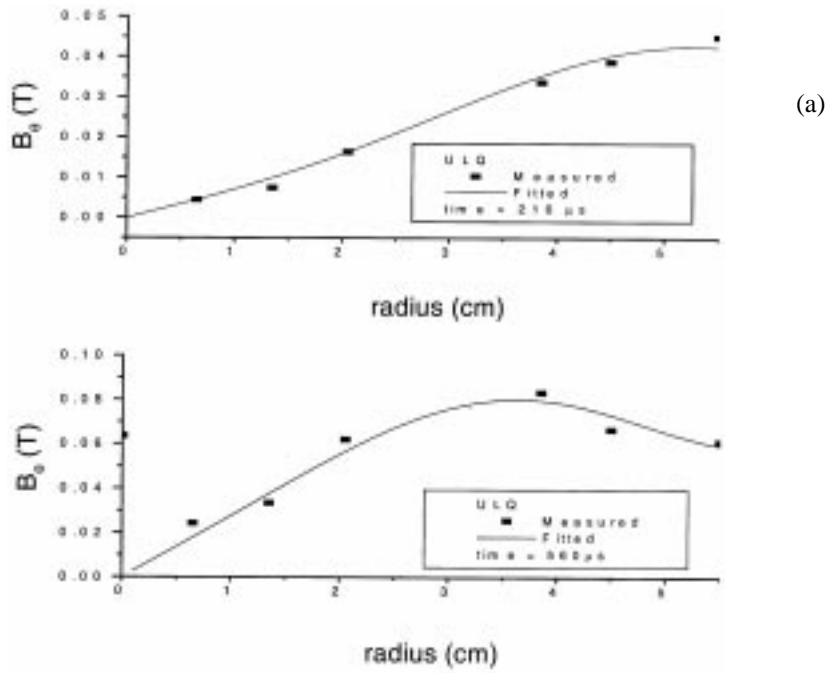


Figure 4a.

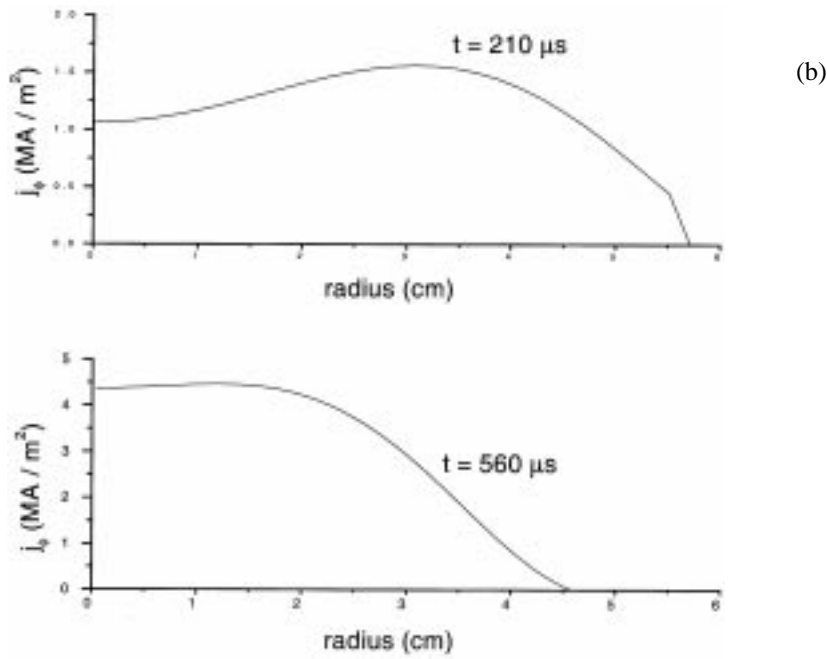
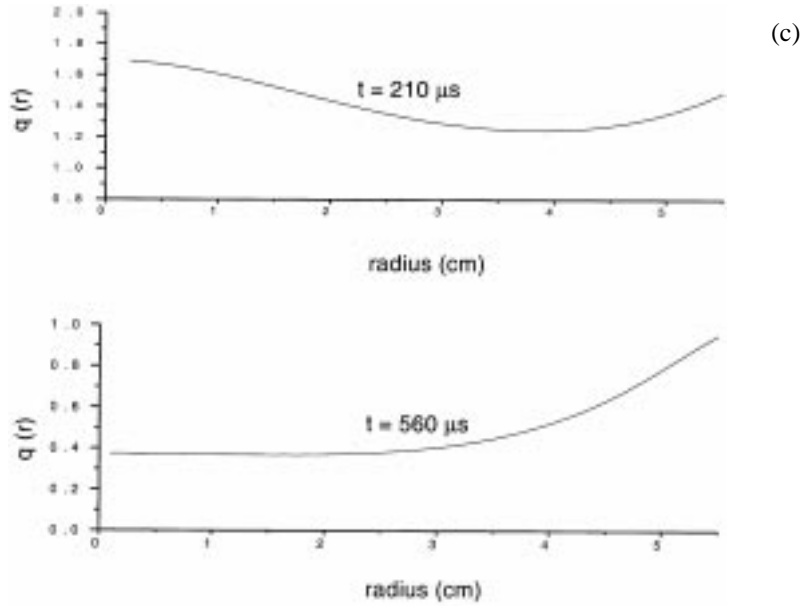


Figure 4b.



**Figure 4.** (a)  $B_\theta$  profiles in the rising phase ( $210 \mu\text{s}$  and  $560 \mu\text{s}$ ) of the ULQ discharge. (b)  $j_\phi$  profiles in the rising phase of the ULQ discharge. (c)  $q$  profiles in the rising phase of the ULQ discharge.

**Table 1.** Growth rate of MHD modes at the early rising phase.

$m/n$	Time span ( $\mu\text{s}$ )	$j_\phi$	$q_0$	$q_a$	Average growth time ( $\mu\text{s}$ )
3/1	70–95	Hollow	3.69–2.67	4.68–3.25	$\geq 50$
2/1	120–150	Hollow	2.52–2.25	2.69–2.10	$\geq 15$

**Table 2.** Growth rate of MHD modes before the positive jump of the loop voltage.

$m/n$	Time span ( $\mu\text{s}$ )	$j_\phi$	$q_0$	$q_a$	Average growth time ( $\mu\text{s}$ )
3/2	160–210	Less hollow	2.14–1.68	1.96–1.48	$\geq 20$
1/1	230–300	Less hollow	1.35–1.33	1.37–1.17	$\geq 10$

It is seen from table 1, in the early rising phase of the discharge, that most of the modes are stable except 3/1 and 2/1. Their average growth times are  $\geq 50 \mu\text{s}$  and  $\geq 15 \mu\text{s}$  respectively. The time for which they reside inside the plasma is  $25 \mu\text{s}$  and  $30 \mu\text{s}$  respectively. So, these growth times are large in comparison to the time span for which they stay inside the plasma. Before the occurrence of the positive spike in the loop voltage (results are given in table 2), only 3/2 and 1/1 modes are found to grow. Their average growth times are

**Table 3.** Growth rate of MHD modes around the positive jump of the loop voltage.

$m/n$	Time span ( $\mu\text{s}$ )	$j_\phi$	$q_0$	$q_a$	Average growth time ( $\mu\text{s}$ )
1/1	300–330	Parabolic	1.33–1.08	1.17–1.12	$\geq 10$
4/5	350–500	Parabolic	0.87–0.55	1.07–1.02	Stable
2/3	400–500	Parabolic	0.66–0.55	0.97–1.02	Stable

$\geq 20 \mu\text{s}$  and  $\geq 10 \mu\text{s}$  respectively. Since the 3/2 mode remains inside the plasma for a relatively short period of time ( $\approx 50 \mu\text{s}$ ), this mode is likely to affect the evolution only to a small extent. However, the same is not true for 1/1 mode. In fact, this mode is found to grow even after this period and up to  $330 \mu\text{s}$  (as shown in table 3) with a similar average growth rate. As a result, this mode is likely to have a very important influence in the overall temporal evolution of the plasma discharge. The positive spike in the loop voltage occurs during this period of time (255–355  $\mu\text{s}$ ), the largest spike being observed at  $\approx 325 \mu\text{s}$ . Thus, it seems that the 1/1 mode was the most probable cause behind the sudden positive surge in the loop voltage. After the positive spikes, the discharge enters into the ULQ regime, so the presence of the 1/1 mode is not very much relevant. This analysis supports the second conjecture except for the 1/1 mode made above and the results obtained experimentally.

### 3. Conclusions

It is possible to access the low  $q_a$  regime (both VLQ and ULQ) in the SINP tokamak by adopting the method of fast current rise. The other important factors are the low  $B_t$ , low  $a_p$  and high gas filling pressure. The setting up process is also believed to be aided by some other factors like presence of the conducting shell and presence of the low  $Z$  impurities. Analysis of the experimental data has yielded various interesting and important relations between several plasma parameters which need to be satisfied in order to set-up low  $q_a$  discharges. An array of internal magnetic probe has been designed and fabricated and used to estimate the  $j_\phi(r)$  profile and other internal details of the plasma. It is seen that the  $j_\phi(r)$  profile remains hollow in the initial phase of the discharge and becomes parabolic after a positive spike in the loop voltage. In the ULQ discharge, the hollow  $j_\phi(r)$  is sustained for a longer time than in the VLQ and NQ discharges. The current penetration in the low  $q_a$  discharges takes time of the order of the resistive diffusion time. The positive spike in the loop voltage and the current penetration are found to be related to the growth of MHD instabilities. The time scale  $\tau_R$  is one of the most important time scales in relation to the accessibility of low  $q_a$  discharges. The results obtained from the resistive stability analysis have been found to corroborate the above conclusions. However, to complete the investigation we need to know the temperature and density profiles of the low  $q_a$  discharges. Detailed numerical modeling will also help in understanding the underlying physical processes. Some of these works have been started already [17] and others will be considered for future investigations.

## **Acknowledgement**

This article was presented at the 14th National Symposium on Plasma Science and Technology, Amritsar.

## **References**

- [1] R K Paul, A N Sekar Iyengar and A K Hui, *Nucl. Fusion* **38**, 1381 (1998)
- [2] A N Sekar Iyengar, S K Majumdar, J Basu, R K Paul, R Pal and S Chowdhury, *Pramana – J. Phys.* **39**, 181 (1992)
- [3] A N S Iyengar, R Pal, S K Majumdar and J Basu, *Indian J. Phys.* **B66(5&6)**, 515 (1992)
- [4] S Lahiri, A N Sekar Iyengar, S Mukhopadhyay and R Pal, *Nucl. Fusion* **36**, 254 (1996)
- [5] S V Mirnov and I B Semenov, *Sov. Phys. JETP* **33**, 1134 (1971)
- [6] TIFR Group, *Nucl. Fusion* **24**, 784 (1984)
- [7] DIVA Group, *Nucl. Fusion* **20**, 271 (1980)
- [8] H Yamada, K Kusano and Y Kamada, *Nucl. Fusion* **27**, 1169 (1987)
- [9] H Y W Tsui, R J La Haye and J A Cunnane, *Nucl. Fusion* **30**, 59 (1990)
- [10] Y Kamada, T Fujita, Y Murakami, T Ohira, K Saitoh, Y Fuke, M Utsumi, Z Yoshida and N Inoue, *Nucl. Fusion* **29**, 713 (1989)
- [11] P L Taylor, R J La Haye, M J Schaffer, T Tamano, N Inoue, Z Yoshida and Y Kamada, *Nucl. Fusion* **29**, 92 (1989)
- [12] S Lahiri, S Mukhopadhyay, A N Sekar Iyengar and R Pal, *IEEE Trans. Plasma Sci.* **25**, 509 (1997)
- [13] Z Yoshida, Y Murakami, H Morimoto, J Matsui, D Nagahara, S Takeji and N Inoue, *Nucl. Fusion* **30**, 762 (1990)
- [14] S Lahiri, A N Sekar Iyengar, S Mukhopadhyay and R Pal, *PLASMA-95 Proc.* (1996) 231
- [15] A N Sekar Iyengar, R Pal, S Lahiri and S Mukhopadhyay, *Nucl. Fusion* **38**, 1177 (1998)
- [16] D Brotherton-Ratcliffe and I H Hutchinson, *CLM-R* (1984) 246
- [17] S Lahiri, S Mukhopadhyay, A N Sekar Iyengar and R Pal, *Pramana – J. Phys.* **56**, 615 (2001)